Electronic Supplementary Material (ESI) for Journal of Materials Chemistry B.

Supporting Information

Effective control of the intrinsic DNA morphology by photosensitive polyamines

Marco Deiana,[a] Ziemowit Pokladek,[b] Katarzyna Matczyszyn,[a,*] Piotr Mlynarz,[b] Malcolm Buckle,[c] and Marek Samoc[a]

[a] Advanced Materials Engineering and Modelling Group, Faculty of Chemistry, Wroclaw University of Science and Technology, Wyb. Wyspianskiego 27, 50-370 Wroclaw (Poland)
[b] Department of Bioorganic Chemistry, Faculty of Chemistry, Wroclaw University of Science and Technology, Wyb. Wyspianskiego 27, 50-370 Wroclaw (Poland)
[c] LBPA, ENS Cachan, CNRS, Université Paris-Saclay, 61 Avenue du Président Wilson, F-94235, Cachan (France)

*E-mail: *katarzyna.matczyszyn@pwr.wroc.pl

Table of Contents:

Synthesis

NMR-spectra were recorded on a Bruker Avance™ 600 MHz spectrometer. Mass spectra were conducted with a WATERS LCT Premier XE mass spectrometer (ESI). Unless otherwise noted, all reactions were carried out under normal conditions. Materials and solvents obtained from commercial suppliers were used without further purification.

Synthesis of **1**

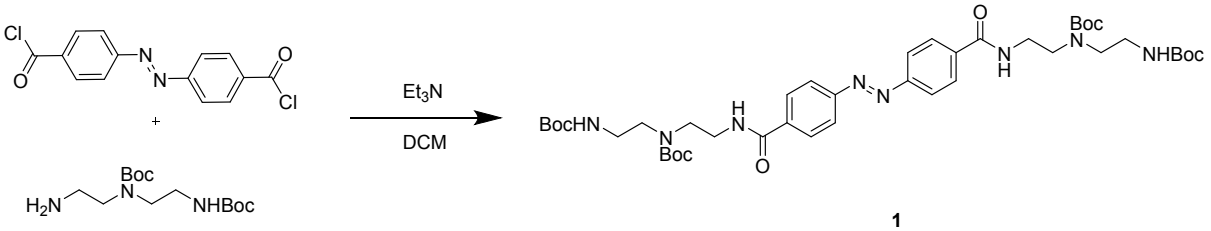

1

To dry dichloromethane (10 mL) solution of 1,4-Bis-boc-1,4,7-triazaheptane (0.3 g,0.99 mmol, 2 eq.) and triethylamine (0.2g, 1.98 mmol, 4 eq), Azobenzene-4,4′-dicarbonyl dichloride was added (0.15 g, 0.495 mmol, 1eq.) and the reaction mixture was stirred overnight. The solvent was evaporated under reduced pressure and the product was purified with column chromatography on silica using EtOAc to afford **1** as orange powder (0.25g, 60%).

^{1}H-NMR ($CDCl_3$,600 MHz) *δ*: 8.11 – 7.84 (m, 8H), 7.72 (s, 2H), 4.90 (s, 2H), 3.66 – 3.47 (m, 8H), 3.39 – 3.19 (m, 8H), 1.51 – 1.34 (m, 36H).

^{13}C-NMR ($CDCl_3$, 75 MHz) *δ*: 166.87, 157.65, 154.23, 136.58, 128.30, 123.11, 79.66, 47.97, 40.92, 39.64, 28.55, 28.50.

HRMS m/z (ESI): Required $[M+Na]^+$: 863.4643 Found: 863.4649

Synthesis of **2**

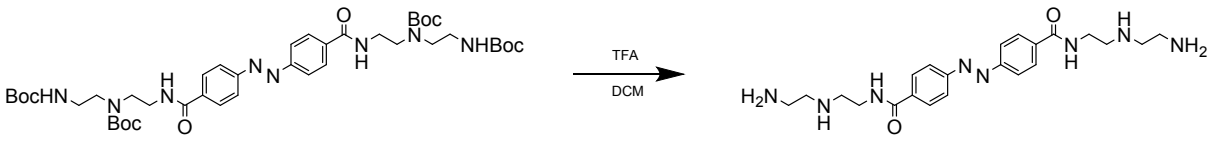

1 2

Compound **1** (0.25g, 0.296 mmol, 1 eq.) was dissolved in DCM (5 mL) and TFA (1mL) was added then stirred overnight. Solvent was removed under reduced pressure and obtained orange residue was dissolved in DCM (15mL) and washed with saturated $NaHCO_3$ solution (3x15mL). The organic layer was dried over $MgSO_4$, filtrated, and evaporated under reduced pressure affording **2** as TFA salt in form of red semi-solid (0.225 g, 85%)

^{1}H NMR (601 MHz, D_2O δ: 7.95 (d, *J* = 8.4 Hz, 4H), 7.87 (d, *J* = 8.4 Hz, 4H), 3.83 (t, *J* = 5.6 Hz, 4H), 3.68 – 3.63 (m, 8H), 3.60 (t, *J* = 7.0 Hz, 4H), 3.53 – 3.47 (m, 8H).

^{13}C NMR (151 MHz, D_2O) δ: 173.2, 156.9, 138.2, 131.5, 125.9, 51.2, 47.7, 46.6, 46.2, 39.4, 38.3.

HRMS m/z (ESI): Required $[M+H]^+$ 441.2726 Found 441.2738

Synthesis of **3**

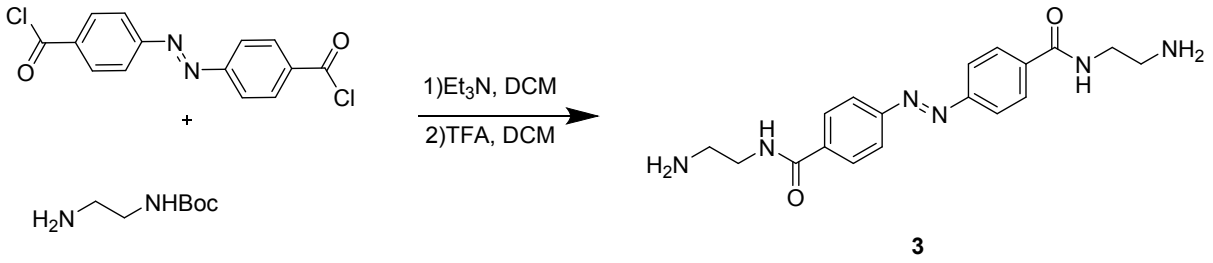

3

To dry dichloromethane (10 mL) solution of N-Boc-ethylenediamine (0.23g, 1.4 mmol, 2.2 eq) and triethylamine (0.45mL, 12.7 mmol ,5 eq.), Azobenzene-4,4′-dicarbonyl dichloride was added (0.2g, 0.65 mmol, 1 eq.) and the reaction mixture was stirred overnight. The red solid was filtered and washed with DCM (20 mL) and dried overnight at high vacuum. Successively, the solid was suspended in DCM (5 mL) and TFA (1 mL) was added and the reaction was stirred overnight. Finally, the solvent was evaporated under reduced pressure affording **3** as a TFA salt in form of red powder (0.41g, 85%).

^{1}H NMR (601 MHz, D_2O) δ:7.92 (d, *J* = 8.1 Hz, 2H), 7.86 (d, *J* = 8.1 Hz, 4H), 3.73 (t, *J* = 5.7 Hz, 4H), 3.30 (t, *J* = 5.7 Hz, 4H).

^{13}C NMR (151 MHz, D_2O) δ: 173.19, 156.90, 138.45 131.50, 125.84, 42.26, 40.42.

HRMS m/z (ESI): Required: $[M+H]^+$: 355.1883 Found:355.1869

Hill plots

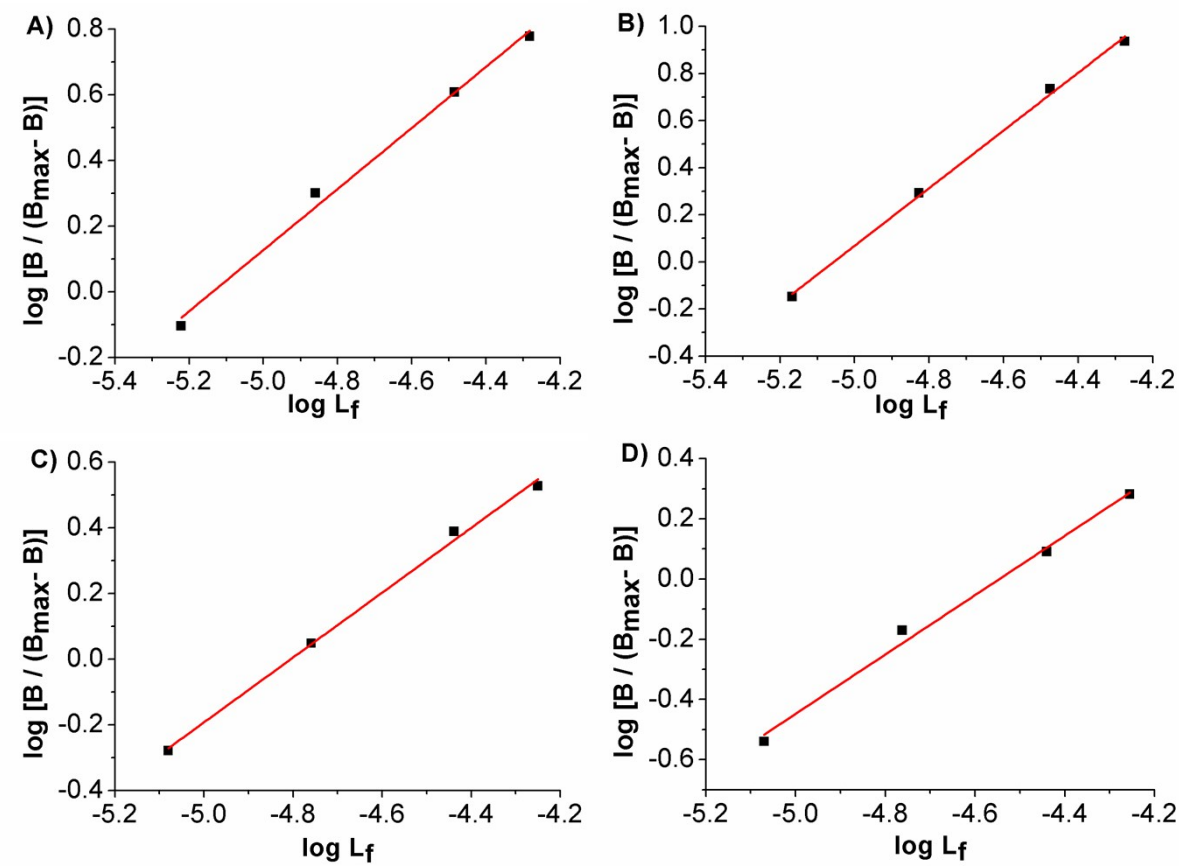

Figure S1. Hill plots for the binding of: **(A) bis-Azo-3N** *trans*-DNA, **(B) bis-Azo-2N** *trans*-DNA, **(C) bis-Azo-3N** *cis*-DNA and **(D) bis-Azo-2N** *cis*-DNA. B is the bound ligand, B_{max} is the total receptor concentration and L_f is the free ligand concentration.

Van't Hoff plots for the determination of the thermodynamic parameters (ΔH, ΔS and ΔG)

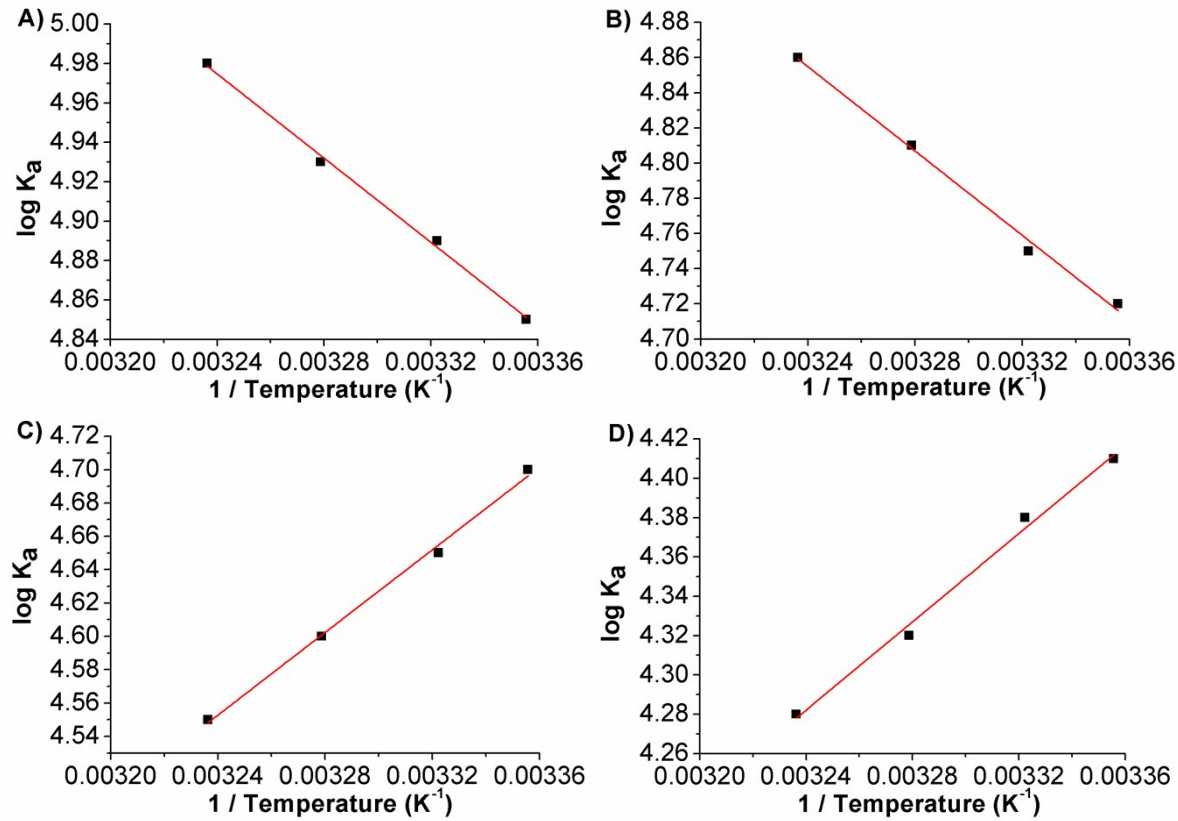

Figure S2. Van't Hoff plots for the binding of **(A) bis-Azo-3N** *trans*, **(B) bis-Azo-2N** *trans*, **(C) bis-Azo-3N** *cis* and **(D) bis-Azo-2N** *cis* to DNA. K_a is the overall binding constant for the photochrome-DNA systems calculated at 298, 301, 305 and 309 K.

Fourier transform infrared (FT-IR) spectroscopy

The FT-IR spectra of free salmon sperm DNA and the relative structural variations caused by photochromes in both their conformations were studied in aqueous solution (pH 7.25) at different DNA / Azobenzene molar ratios (Figure S3 and S4 A-D and Figure S5 A-D). The occurrence of the interaction can be deduced by comparing the individual DNA and the azobenzene derivatives spectra with those of the Azobenzene-DNA complex. The FT-IR spectrum of the free DNA, shown in Figure S3, is mainly constituted of bands confined in the 1800 - 400 cm^{-1} region arising from the ring vibrations of the nitrogenous bases (C=O, C=N), symmetric and asymmetric stretching vibrations of the phosphate groups (PO_2) and stretching of the phosphate-ribose diester linkage (C-O, P-O). The band at 1701 cm^{-1} is due to the in-plane stretching vibrations of guanine (G) while the band at 1652 cm^{-1} is attributable primarily to the

vibrations of C_4=O of thymine (T).[1] The bands at 1579 and 1527 cm^{-1} can be ascribed to in-plane stretching vibrations of C8=N7 of purine ring and cytosine and guanine residues.[1b,2] The vibrational bands at 1606, 1488 and 1417 cm^{-1} are typical of adenine (A), cytosine (C), and ring vibrations of guanine (G) bases, respectively.[1,2] The band at 1456 cm^{-1} is assigned to C-N glycosyl bond.[3] The bands at 1242, 1093, 1068 and 962 cm^{-1} are related to the asymmetric and symmetric stretching vibration of phosphate group.[4] Moderate strength peaks are located at 1370, 1294, 889, 833, 781 and 730 cm^{-1} corresponding to the stretching of C-O, P-O (phosphate-ribose diester linkage) and N-H out of plane bending vibrations.[5]

The FT-IR spectra of the photochromes in *trans* and *cis* conformation are shown in Figure S3. The spectra are very similar and present a strong band at 1675 cm^{-1} that can be assigned to the amide C=O stretching. The bands at 1570 and 1542 cm^{-1} can be attributed to the C=C stretching vibrations of the benzene rings. The peak at 1494 cm^{-1} arises from both the stretching of the C-N and the rocking of the C-H groups. The band at 1459 cm^{-1} can be ascribed to the stretching vibration of the methylene spacer groups. The characteristic azo (N=N) bond stretching vibration is found at 1436 cm^{-1}. The bands at 1201 and 1140 cm^{-1} are due to C-N_{azo} and C-N stretching vibrations, respectively. Additional bands are found at 840, 800, 777 and 723 cm^{-1} presumably assigned to the C-H wagging of the aromatic rings.

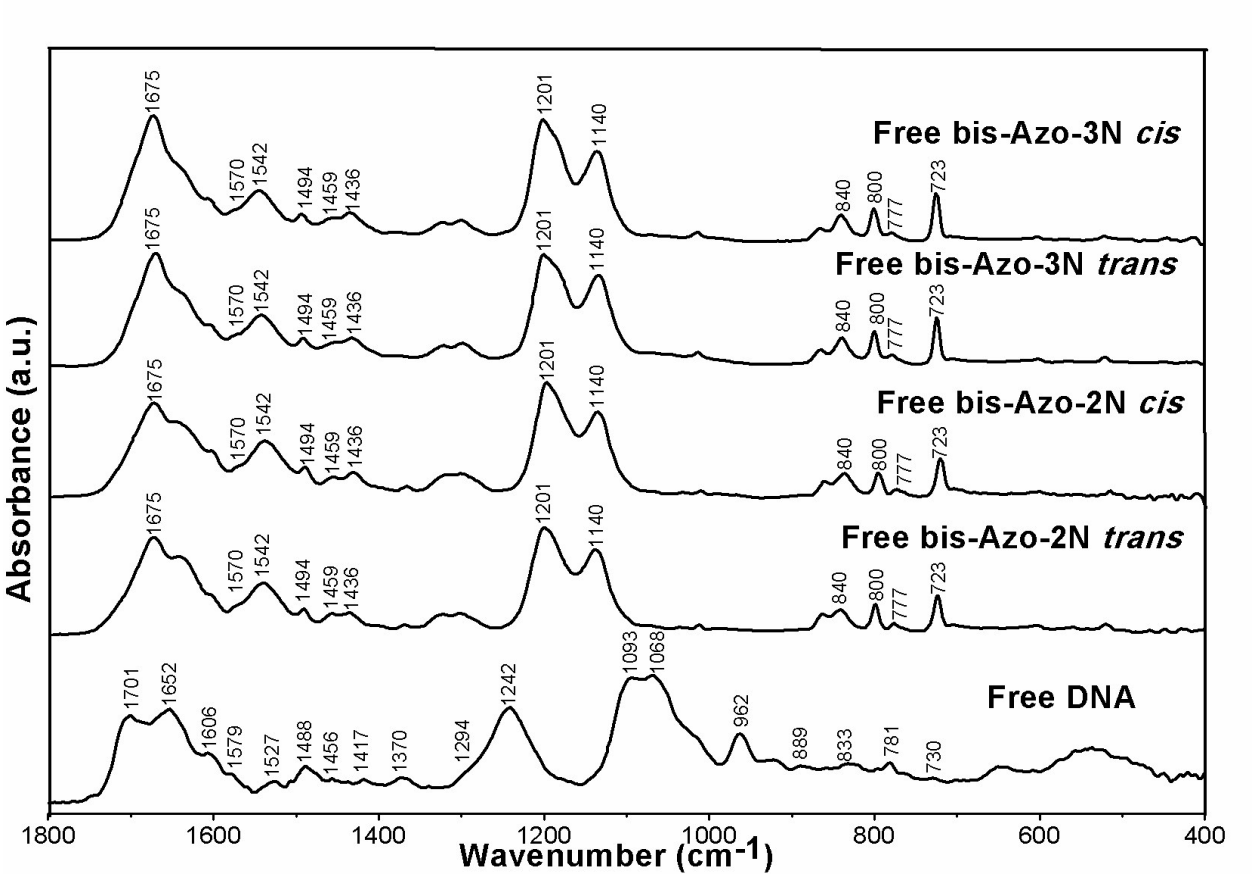

Figure S3. FT-IR spectra of free DNA and the photochromes in their isomeric forms in the 1800-400 cm^{-1} region.

Difference FTIR spectra:

[(*ds*-DNA solution + Azobenzene) – Azobenzene solution]

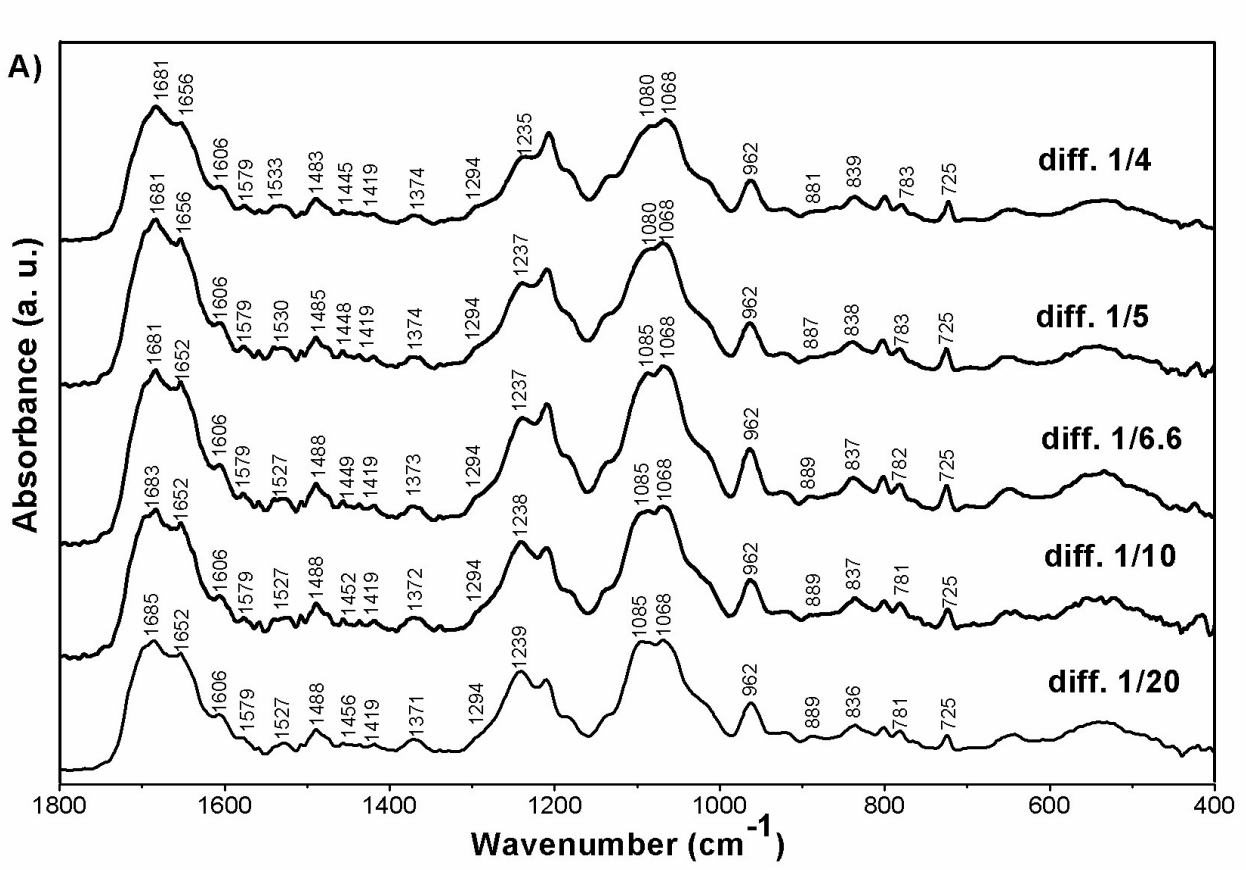

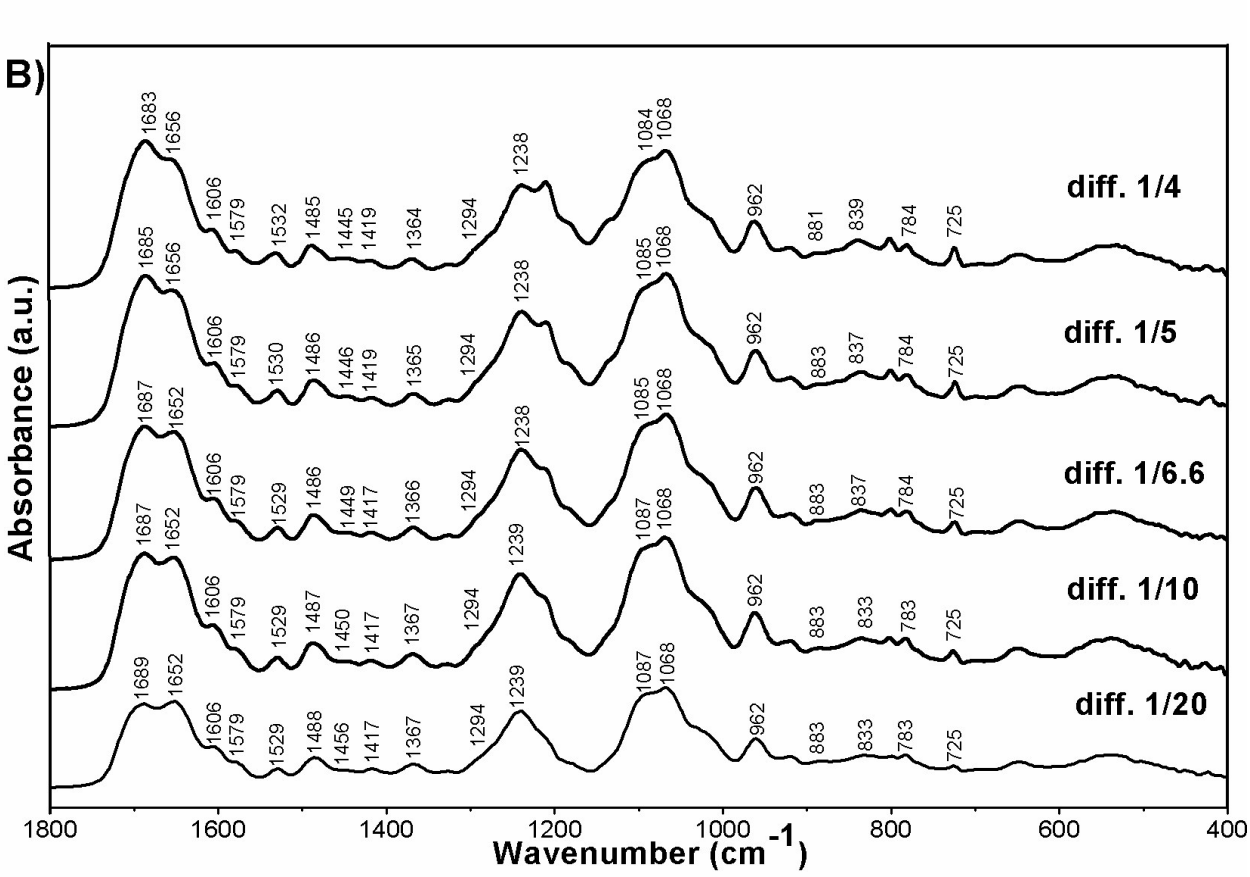
B)
Absorbance (a.u.)
diff. 1/4
diff. 1/5
diff. 1/6.6
diff. 1/10
diff. 1/20
Wavenumber (cm-1)

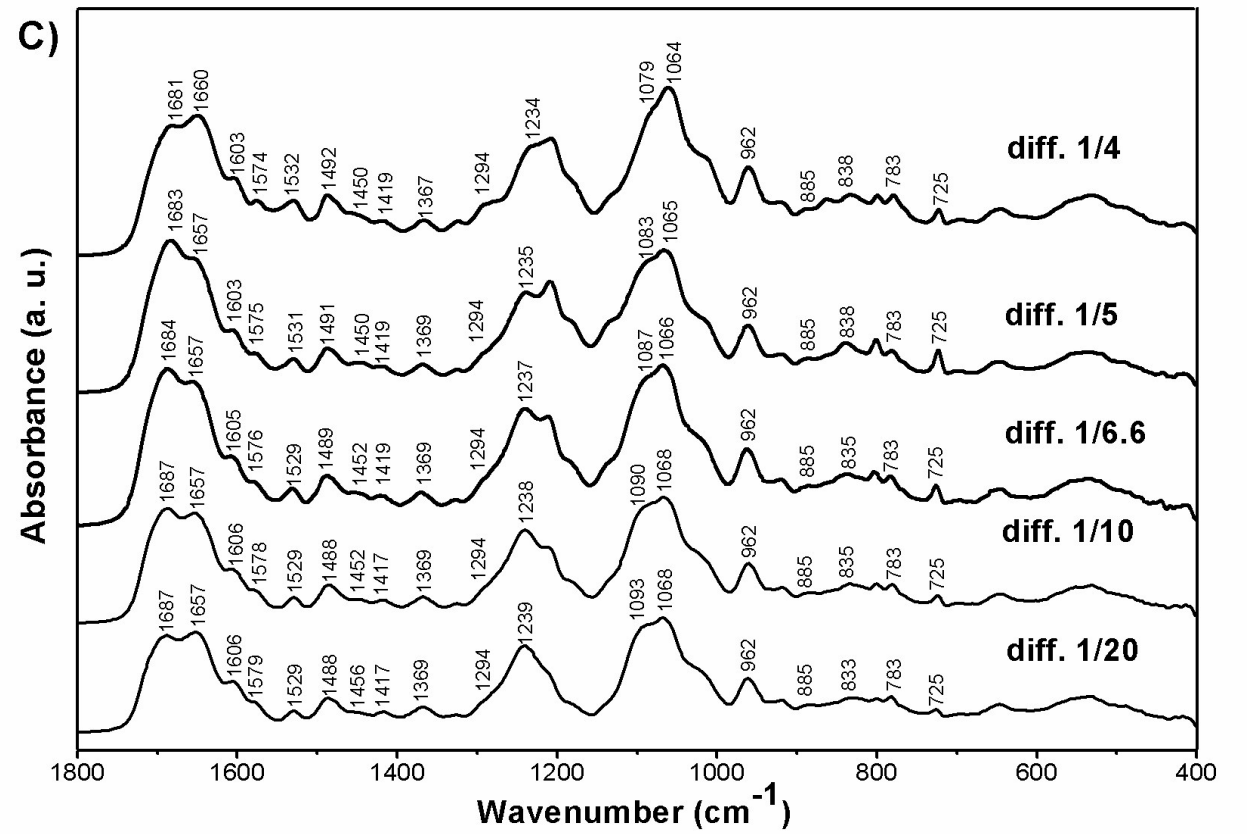
C)
Absorbance (a. u.)
diff. 1/4
diff. 1/5
diff. 1/6.6
diff. 1/10
diff. 1/20
Wavenumber (cm-1)

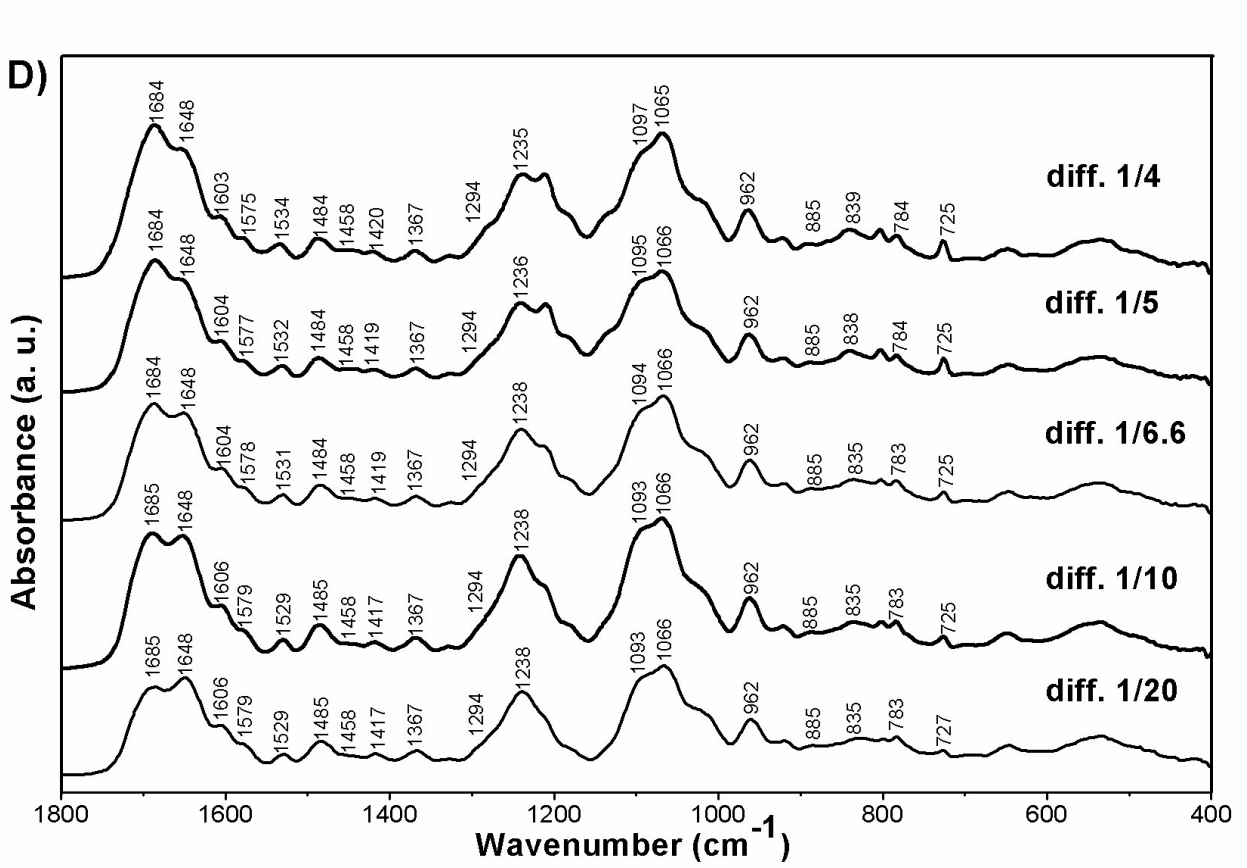

Figure S4. (A) Difference FT-IR spectra [(DNA solution + **bis-Azo-3N** *trans*) – **bis-Azo-3N** *trans*], **(B)** Difference FT-IR spectra [(DNA solution + **bis-Azo-2N** *trans*) – **bis-Azo-2N** *trans*], **(C)** Difference FT-IR spectra [(DNA solution + **bis-Azo-3N** *cis*) – **bis-Azo-3N** *cis*] and **(D)** Difference FT-IR spectra [(DNA solution + **bis-Azo-2N** *cis*) – **bis-Azo-2N** *cis*] at different molar ratios in the 1800-400 cm^{-1} region.

Plots of the intensity ratio variations of the main FTIR bands involved in the complexation process

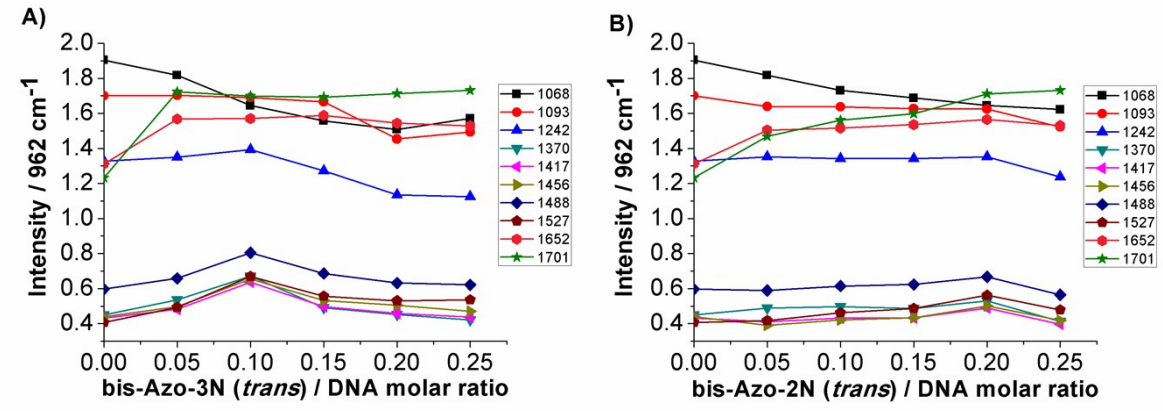

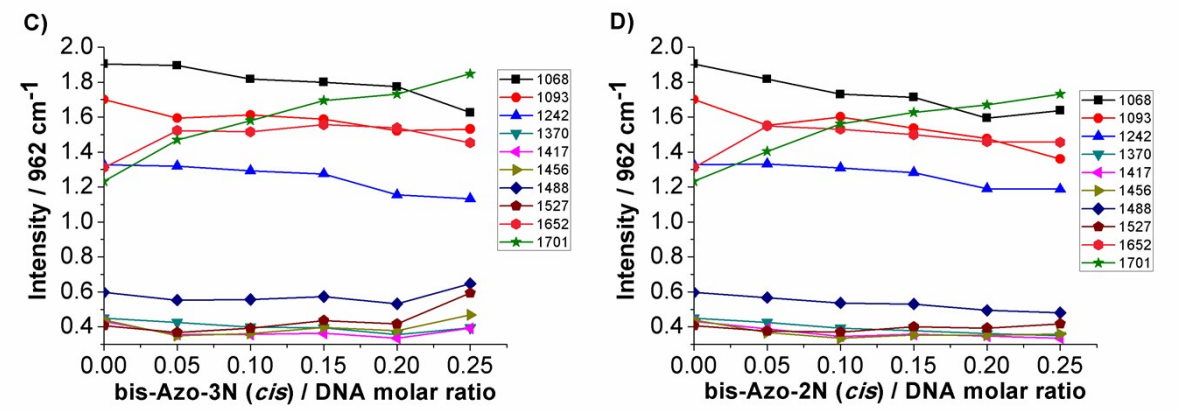

Figure S5. Plots of the intensity ratio variations as a function of **(A) bis-Azo-3N** *trans*-DNA, **(B) bis-Azo-2N** *trans*-DNA, **(C) bis-Azo-3N** *cis*-DNA and **(D) bis-Azo-2N** *cis*-DNA molar ratio.

Plots of the ellipticity variations of the main CD and ICD bands involved in the complexation process

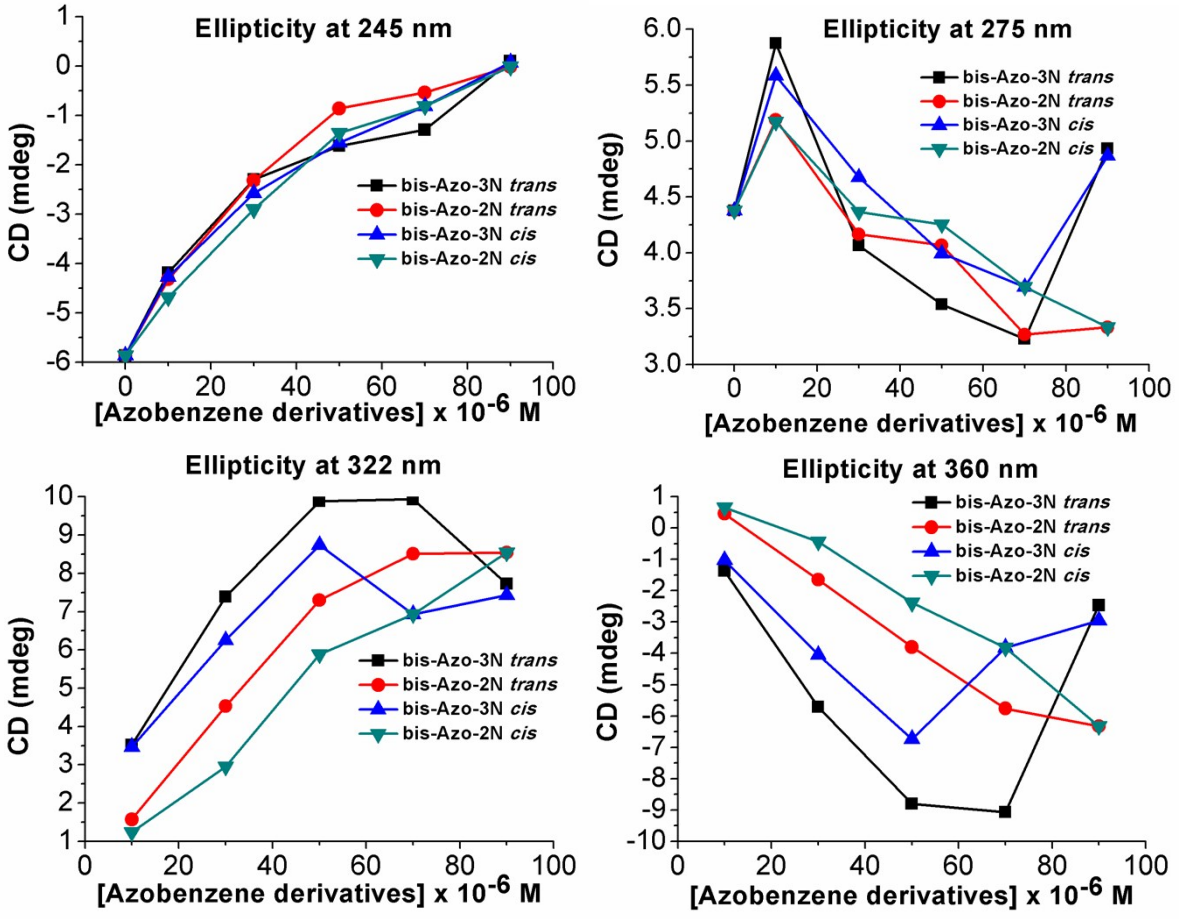

Figure S6. The comparative graphs represent the changes in DNA molar ellipticity at 245, 275, 322 and 360 nm.

Plots of the apparent association constants at various salt concentrations

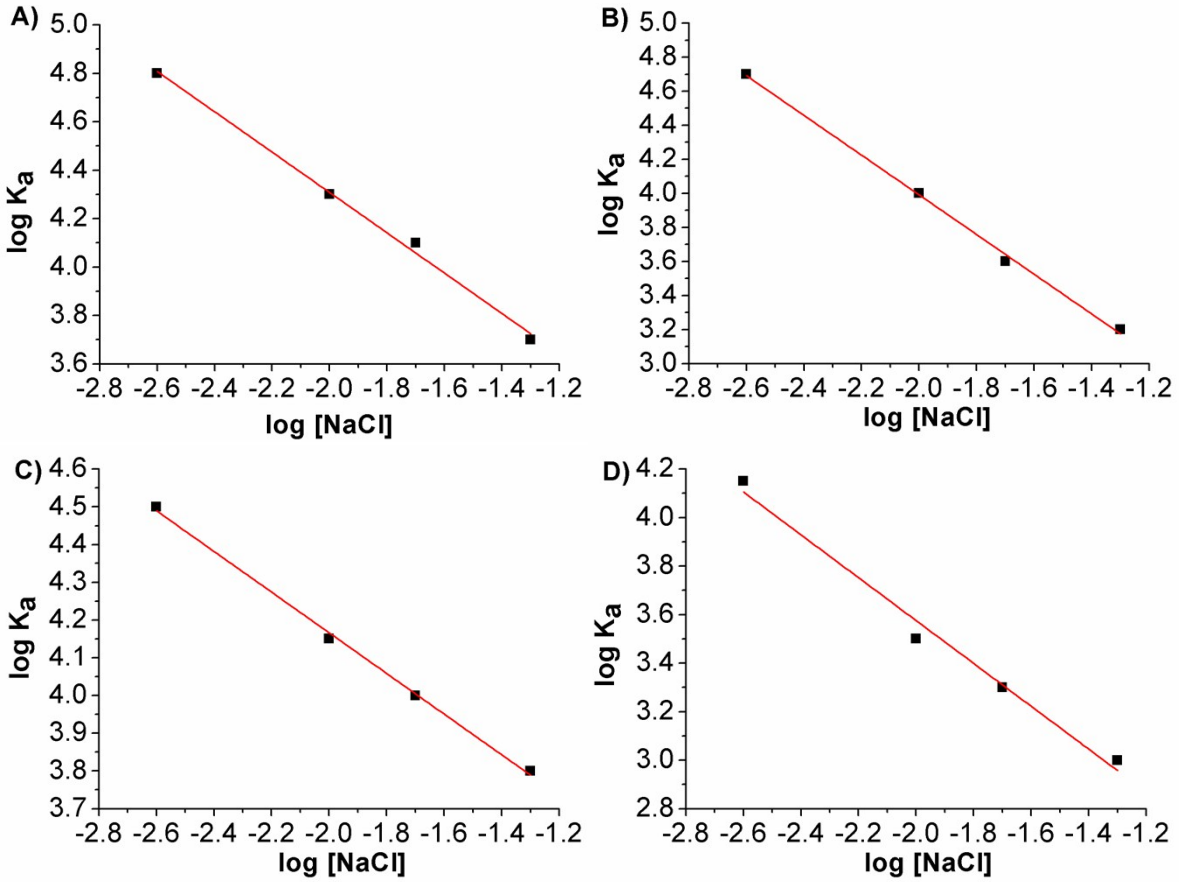

Figure S7. Dependence of the observed binding constant (K_a) of **(A) bis-Azo-3N** *trans*-DNA, **(B) bis-Azo-2N** *trans*-DNA, **(C) bis-Azo-3N** *cis*-DNA and **(D) bis-Azo-2N** *cis*-DNA *versus* the concentration of sodium chloride.

Polyamine charges

The amine pK_a values were determined by using the MarvinSketch software. Based on such values, it was possible to determine the charge (n) by using the following equations[6]:

bis-Azo-2N: pK_{a1}: 8.86 and pK_{a2}: 9.46

$$n = \frac{\frac{K_{a1}}{10^{-pH}} + 2}{1 + \frac{K_{a1}}{10^{-pH}} + \frac{K_{a1}K_{a2}}{10^{-2pH}}} \quad (1)$$

bis-Azo-3N: pK_{a1}: 6.58, pK_{a2}: 7.18, pK_{a3}: 9.30 and pK_{a4}: 9.90

$$n = \frac{\frac{K_{a1}K_{a2}K_{a3}}{10^{-3pH}} + 2\frac{K_{a1}K_{a2}}{10^{-2pH}} + 3\frac{K_{a1}}{10^{-pH}} + 4}{1 + \frac{K_{a1}}{10^{-pH}} + \frac{K_{a1}K_{a2}}{10^{-2pH}} + \frac{K_{a1}K_{a2}K_{a3}}{10^{-3pH}} + \frac{K_{a1}K_{a2}K_{a3}K_{a4}}{10^{-4pH}}} \quad (2)$$

giving the values:

$n_{\textbf{bis-Azo-2N}}$: 1.98

$n_{\textbf{bis-Azo-3N}}$: 2.59

References

1) a) D. R. Whelan, K. R. Bambery, P. Heraud, M. J. Tobin, M. Diem, D. McNaughton and B. R. Wood, *Nucleic Acids Res.* 2011, **39**, 5439-5448; b) D. M. Loprete and K. A. Hartman, *Biochemistry* 1993, **32**, 4077-4082.

2) J. F. Neault and H. A. Tajmir-Riahi, *Biophys. J.* 1999, **76**, 2177-2182.

3) S. Agarwal, D. K. Jangir, P. Singh and R. Mehrotra, *J. Photochem. Photobiol. B* 2014, **130**, 281-286.

4) a) R. Marty, C. N. N'soukpoe-Kossi, D. Charbonneau, C. M. Weinert, L. Kreplak and H. A. Tajmir-Riahi, *Nucleic Acids Res.* 2009, **37**, 749–757; b) E. V. Hackl, S.V. Kornilova, L. E. Kapinos, V. V. Andrushchenko, V. L. Galkin, D. N. Grigoriev and Y. P. Blagoi. *J. Mol. Struct.* 1997, **408**, 229-232.

5) B. Rafique, A. M. Khalid, K. Akhtar and A. Jabbar, *Biosens Bioelectron.* 2013, **44**, 21-26.

6) A. Venancio-Marques, A. Bergen, C. Rossi-Gendron, S. Rudiuk and D. Baigl, *ACSnano* 2014, **8**, 3654-3663.